Electronic Supplementary Material (ESI) for Chemical Science.

The ionic liquid-gas outer atomic surface: a low energy ion scattering study

Supplementary Information

Ignacio J. Villar-Garcia[1], Sarah Fearn[1], Gilbert F. De Gregorio[2], Nur L. Ismail[2],
Florence J. V. Gschwend,[3] Alastair J. S. McIntosh[2], Kevin R. J. Lovelock[2]

[1] Department of Materials, Imperial College London.
[2] Department of Chemistry, Imperial College London.
[3] Department of Chemical Engineering, Imperial College London.

Email: kevin.lovelock@imperial.ac.uk
Address: Department of Chemistry
Imperial College London
Exhibition Road, South Kensington
SW7 2AZ
Tel: +44 (0)20 7594 5868

1. Ionic liquids studied in this paper

Abbreviation	Structure	Name
$[C_4C_1Im][CF_3SO_3]$	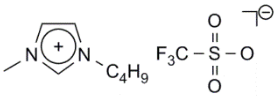	1-butyl-3-methylimidazolium trifluoromethylsulfonate
$[C_4C_1Im][PF_6]$	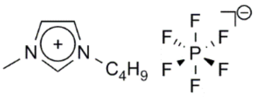	1-butyl-3-methylimidazolium hexafluorophosphate
$[C_4C_1Im][BF_4]$	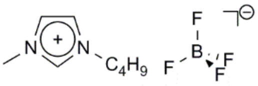	1-butyl-3-methylimidazolium tetrafluoroborate
$[C_2C_1Im][Tf_2N]$	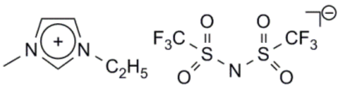	1-ethyl-3-methylimidazolium *bis*[(trifluoromethane)sulfonyl]imide
$[C_4C_1Im][Tf_2N]$	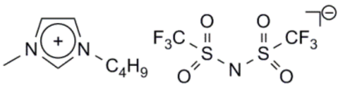	1-butyl-3-methylimidazolium *bis*[(trifluoromethane)sulfonyl]imide
$[C_6C_1Im][Tf_2N]$	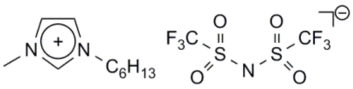	1-hexyl-3-methylimidazolium *bis*[(trifluoromethane)sulfonyl]imide
$[C_8C_1Im][Tf_2N]$	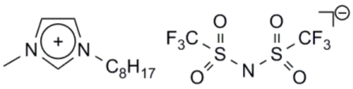	1-octyl-3-methylimidazolium *bis*[(trifluoromethane)sulfonyl]imide
$[C_{12}C_1Im][Tf_2N]$	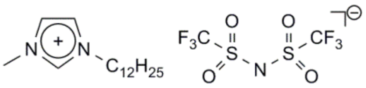	1-dodecyl-3-methylimidazolium *bis*[(trifluoromethane)sulfonyl]imide
$[C_4C_1Pyrr][Tf_2N]$	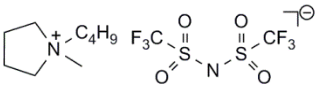	1-butyl-1-methylpyrrolidinium *bis*[(trifluoromethane)sulfonyl]imide
$[N_{4,1,1,1}][Tf_2N]$	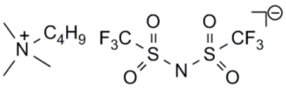	butyl(trimethyl)ammonium *bis*[(trifluoromethane)sulfonyl]imide
$[P_{6,6,6,14}][Tf_2N]$	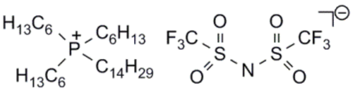	tetradecyl(trihexyl)phosphonium *bis*[(trifluoromethane)sulfonyl]imide
$[P_{6,6,6,14}]Cl$	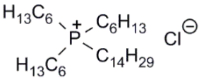	tetradecyl(trihexyl)phosphonium chloride
$[C_8C_1Im]Cl$	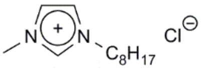	1-octyl-3-methylimidazolium chloride
$[P_{6,6,6,14}][N(CN)_2]$	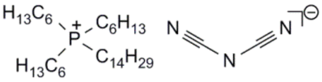	tetradecyl(trihexyl)phosphonium dicyanamide
$[C_2C_1Im][N(CN)_2]$	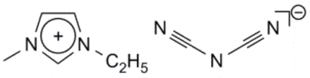	1-ethyl-3-methylimidazolium dicyanamide
$[C_4C_1Im][N(CN)_2]$	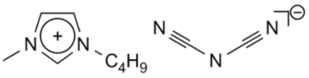	1-butyl-3-methylimidazolium dicyanamide
$[C_2C_1Im][B(CN)_4]$	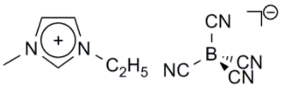	1-ethyl-3-methylimidazolium tetracyanoborate
$[C_4C_1Im][SCN]$	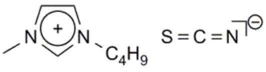	1-butyl-3-methylimidazolium thiocyanate

$[C_4C_1Im][C_0OSO_3]$	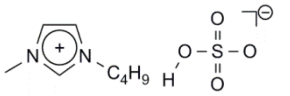	1-butyl-3-methylimidazolium hydrogensulfate
$[C_4C_1Im][C_1OSO_3]$	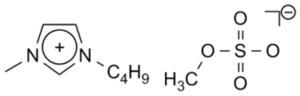	1-butyl-3-methylimidazolium methylsulfate
$[C_4C_1Im][C_8OSO_3]$	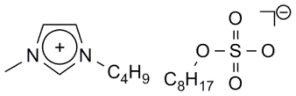	1-butyl-3-methylimidazolium octylsulfate
$[C_2C_1Im][C_1CO_2]$	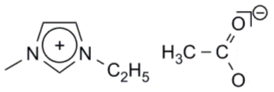	1-ethyl-3-methylimidazolium acetate
$[C_4C_1Im][C_1CO_2]$	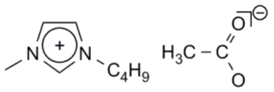	1-butyl-3-methylimidazolium acetate

Table S1. Ionic liquids investigated in this work.

2. Ionic liquid synthesis

The synthesis and analytical data of the ionic liquids synthesised following modified procedures from the literature are presented below:

Synthesis of 1-dodecyl-3-methylimidazolium *bis*[(trifluoromethane)sulfonyl]imide, $[C_{\underline{12}}C_{\underline{1}}Im][Tf_{\underline{2}}N]$:[1]
Lithium *bis*(trifluoromethane)sulfonylimide (6.32 g, 22 mmol) was added to a stirred solution of 1-dodecyl-3-methylimidazolium chloride (6.30 g, 22 mmol) in dichloromethane (100 mL) and water (20 mL) forming a biphasic mixture and left to stir for three days at room temperature. The upper aqueous phase was decanted. The organic phase was then washed with water (2 x 100 mL). The organic phase was then dried over $MgSO_4$ with the solvent removed under reduced pressure and finally *in vacuo* at 55 °C to yield a colourless liquid (9.67 g, 83 %).
^1H NMR (400 MHz, DMSO-d6): δ/ppm, 9.09 (1H, s, NC*H*N), 7.75 (1H, s, NC*H*), 7.69 (1H, s, NC*H*), 4.14 (2H, t, *J*=7.2 Hz, $NC\mathit{H}_2$), 3.84 (3H, s, $NC\mathit{H}_3$), 1.75 (2H, qnt, *J*=6.8 Hz, $NCH_2C\mathit{H}_2$), 1.24 (18H, s, $NCH_2CH_2(C\mathit{H}_2)_9$-) and 3.11 (3H, t, *J*=6.4 Hz, $N(CH_2)_{11}C\mathit{H}_3$).
^{13}C NMR (100 MHz, d6-DMSO): δ/ppm, 136.95, 124.06, 122.72, 121.55, 118.35, 49.23, 36.18, 31.75, 29.83, 29.47, 29.40, 29.27, 29.17, 28.82 and 25.95. *m/z* FAB+ 251 ($[C_{12}C_1Im]^+$, 100%) *m/z* FAB– 280 ($[Tf_2N]^-$ 100%)

Synthesis of 1-butyl-3-methylimidazolium hydrogensulfate $[C_4C_{\underline{1}}im][C_{\underline{0}}OSO_{\underline{3}}]$:[2]
60 g of $[C_4C_1im][MeSO_4]$ (240 mmol) were mixed with 10 mL of distilled H_2O in a three-necked round bottom flask. 3-4 drops of H_2SO_4 were added drop-wise to the solution. The solution was stirred at 165 °C in an open round bottom flask to facilitate the removal of boiling methanol from the solution. The flask was also fitted with a dropping funnel containing distilled water and a thermometer. The solution temperature was monitored and maintained at 165 °C by adding the H_2O drop-wise into the solution. The progress of the reaction was monitored by the disappearance of the methyl peak in ^1H NMR spectrum. After reaction completion the product was dried under vacuum at 50 °C.

^1H-NMR (400 MHz, DMSO-d6) δ: 9.93 (1H, s, $\underline{H}SO_4$), 9.21 (1H, s, $NC\underline{H}N$), 7.82 (1H, t, $CH_3NCHC\underline{H}N$), 7.75 (1H,t, $CH_3NC\underline{H}CHN$), 4.18 (2H, t, $NC\underline{H}_2(CH_2)_2CH_3$), 3.87 (3H, s, N-$C\underline{H}_3$), 1.75 (2H, m,

$NCH_2C\underline{H}_2CH_2CH_3$), 1.20 (2H, m, N-$(CH_2)_2$-$C\underline{H}_2CH_3$) and 0.87 (3H, t, N-$(CH_2)_3$-$C\underline{H}_3$). ^{13}C-NMR (400 MHz, DMSO-d_6) δ: 137.18 ($N2\underline{C}H$), 123.98 ($N\underline{C}H$), 122.74 ($N\underline{C}H$), 48.84 ($N\underline{C}H_2(CH_2)_2CH_3$), 36.06 ($N\underline{C}H_3$), 31.88 (N-$CH_2\underline{C}H_2CH_2CH_3$), 19.16 ($N(CH_2)_2\underline{C}H_2CH_3$) and 13.64 ($N(CH_2)_3\underline{C}H_3$). *ν*(neat)/cm-1 3156 - 3101 (aromatic C-H stretch, m), 2963 (aliphatic C-H stretch, m), 1576 (arom. ring def., m), 1161 (asym. S=O stretch, s) 1021 (sym. S=O stretch, s). *m/z* ($LSIMS^+$) 139 (100%, $[C_4C_1im]^+$), *m/z* ($LSIMS^-$) 97 (100%, $[C_0OSO_3]^-$).

Synthesis 1-butyl-3-methylimidazolium methylsulfate, $[C_4C_1im][C_1OSO_3]$:[2]

Dimethyl sulfate was dried for 24 hours over calcium hydroxide and distilled under vacuum at 80 °C. N-butylimidazole was dried for 24 h over potassium hydroxide and distilled under vacuum. N-butylimidazole (54.2 g, 0.44 moles) was mixed with 70 mL of toluene and the mixture was cooled to 0 °C. Dimethyl sulfate was added dropwise to the stirred solution (55.1 g, 0.44 moles). The reaction was left stirring for one hour until the reaction mixture reached room temperature. The top phase was decanted and the lower phase washed three times with 50 mL toluene. The ionic liquid was dried under vacuum yielding a clear viscous liquid (105.7 g, 97 %).

δH: (400MHz, $CDCl_3$)/ppm 9.11 (1H, s, NC*H*N), 7.77 (1H, s, NC*H*), 7.70 (1H, s, NC*H*), 4.16 (2H, t, *J*= 8 Hz, $CH_2CH_2CH_2CH_3$), 3.85 (3H, s, NC*H*3), 3.37 (3H, s, CH_3-O-S), 1.76 (2H, m, $CH_2CH_2CH_2CH_3$), 1.25 (2H, m, $CH_2CH_2CH_2CH_3$) and 0.9 (3H, t, *J*= 8 Hz, $CH_2CH_2CH_2CH_3$). δC: (100 MHz, DMSO-d6)/ppm 136.73, 123.83, 122.48, 53.01, 48.69, 35.94, 31.84, 18.97 and 13.47. *m/z* (ES+) 139, ($[C_4C_1Im]^+$ 100%). m/z (ES-) 110 ($[C_1OSO_3]^-$ 100%).

3. Ionic liquid-gas *vs*. ionic liquid-vacuum surfaces

We have decided to use ionic liquid-gas surface when there are gas phase collisions above the ionic liquid surface. We have decided to use ionic liquid-vacuum surface when there are no gas phase collisions above the ionic liquid surface. The base pressure in our LEIS chamber is 3×10^{-10} mbar, which corresponds to a gas phase mean free path of ~30 km. Clearly, no gas phase collisions above the ionic liquid surface occur, and so we use ionic liquid-vacuum surface to refer to the samples we investigated in these LEIS experiments.

4. Predicting E_F

Based upon the laws of classical mechanics, the following Equation can be determined:

$$\frac{E_F}{E_0} = \left(\frac{(m_2^2 - m_1^2 \,.\, \sin^2\theta)^{½} + m_1 \,.\, \cos\theta}{m_2 + m_1} \right)^2 \qquad \text{(S1)}$$

where E_0 is the kinetic energy of the incoming ion, E_F is the kinetic energy of the scattered ion, θ is the scattering angle, m_1 is the atomic mass of the incident ion (in our case, for He^+) and m_2 is the atomic mass of the scattering (target) atom in the sample.[3, 4] If an element is present at the outer surface in significant concentration a Gaussian-shaped peak is observed at a characteristic energy that can be predicted using Equation 1 (commonly labelled as the surface peak for that element).

Table S1 gives the predicted and recorded peak energies. However, due to the He^+-target atom collision not being entirely elastic, the observed and predicted energies do not match exactly, *i.e*. the energy observed for a surface peak is always at lower energy than energy predicted.[3, 4]

Element	Molar mass / g mol^{-1}	E_F(predicted) from Equation S1 / eV	E_F(measured) / eV
B	10.8	726	Not detected
C	12.0	848	786 to 819
N	14.0	1028	987 to 1003
O	16.0	1183	1135 to 1143
F	19.0	1377	1326 to 1330
Si	28.1	1780	1704 to 1714
P	31.0	1870	1783 to 1787
S	32.1	1901	1788 to 1835
Cl	35.5	1986	1897 tob 1904

Table S2. E_F(predicted) and E_F(measured) for He^+ (4 g mol^{-1}) at $\theta = 145°$ and E_0 = 3 keV.

5. Static conditions for LEIS for ionic liquids

It is important to demonstrate that our LEIS results are representative of the undamaged ionic liquid surface. The 3 keV He^+ ions striking the outer ionic liquid surface have the potential to cause localised damage to the ionic liquid surface through both sputtering and changes in molecular structure. For our LEIS experiments, the number of He^+ ions that strike the ionic liquid surface during an experiment ranged from 2.0×10^{15} ions cm^{-2} to 1.2×10^{16} ions cm^{-2}; the experiments were carried over time periods ranging from 30 minutes to 120 minutes, with an average flux of ~3.3×10^{12} ions cm^{-2} s^{-1}. These ion totals are significantly greater than the maximum recommended dose for static conditions on solid organic samples such as polymers, 10^{13} ions cm^{-2} (for metal samples the maximum recommended dose is 10^{15} ions cm^{-2}).[5] The sputter yield for our conditions is expected to be of the order of 0.1 atoms per incident He^+ ion, meaning the total sputter yield for an experiment is ~10^{15} atoms cm^{-2}. It has been concluded previously using XPS that ionic liquid surfaces are not significantly damaged after bombardment with Ar^+ ions (~1 keV).[6, 7] We have made similar observations using LEIS; clean LEIS spectra before and after Ar^+ bombardment are the same within the error of the experiment. Larger ions such as Ar^+ are expected to cause greater damage to a surface than He^+.[5] These observations demonstrate that any damage products produced by Ar^+ bombardment of the ionic liquid surface are: sputter away, vaporise away, or diffuse into bulk ionic liquid. As a typical surface is expected to contain ~5×10^{15} ions cm^{-2}, in a typical experiment, we expect that each surface atom would be struck on average once per experiment. Lísal *et al*. used intrinsic analysis MD simulations to investigate the residence time for ions in $[C_nC_1Im][Tf_2N]$ (n = 4, 6, 8).[8] The residence time for an ionic liquid ion in the surface layer was determined as between 0.1 ns and 1 ns.[8] Therefore, the probability of probing ionic liquid damage products at the surface of ionic liquids is minimal, as any damage products remaining in the liquid phase will diffuse away from the outer surface before another He^+ ion strikes that same position. Therefore, the contribution of these products to the final signal is insignificant and consequently, during our LEIS experiments we are always analysing the pristine and undamaged ionic liquid surface.

6. Diamond reference LEIS spectra

As reference samples, we have studied clean diamond and oxygen plasma-treated diamond (Figure S1) at the same instrument conditions used to investigate ionic liquids. From these two samples, we obtained the peak energies for outer surface carbon and oxygen as E_F = 809 eV and E_F = 1142 eV respectively. For nitrogen, fluorine, sulfur, chlorine and phosphorus, we use ionic liquids to obtain peak energies for outer surface atoms (see Section 3.3), as a Gaussian peak was observed for each of these elements for at least one ionic liquid.

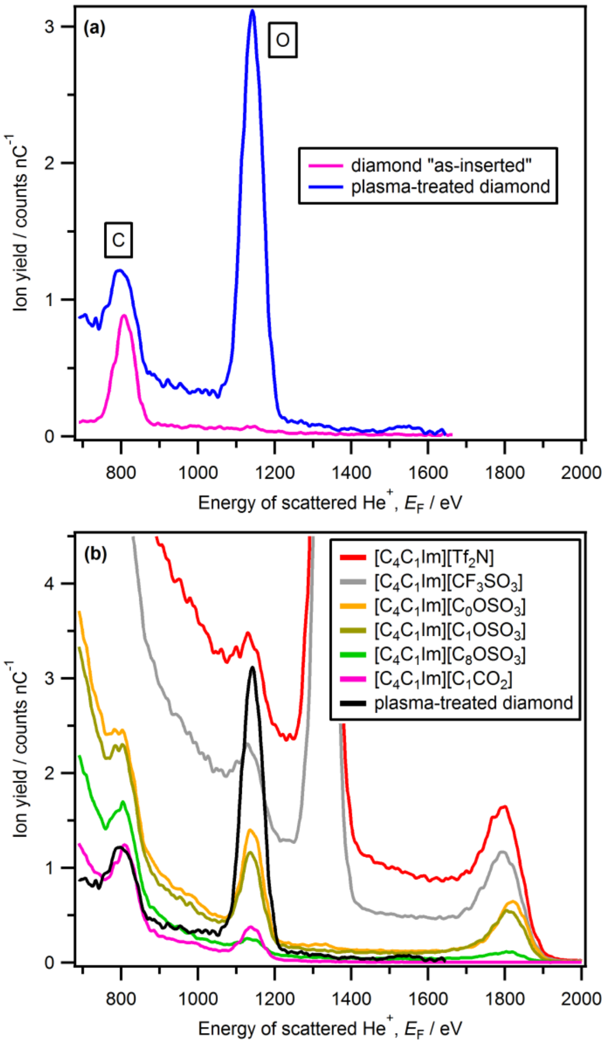

Figure S1. LEIS spectra ($^4He^+$, E_0 = 3 keV) for: (a) diamond and plasma-treated diamond, (b) diamond and plasma-treated diamond and six [C_4C_1Im][A] ionic liquids.

7. Elemental quantification

The measured surface peak area of an element is related to the amount of that element present at the outer atomic surface by:

$$Y_\mathrm{i} = N_\mathrm{i} \,.\, P_\mathrm{i}^+ \,.\, d\sigma_\mathrm{i}/d\Omega \,.\, \frac{I_\mathrm{p}}{e} \,.\, t \,.\, \xi \,.\, R = N_\mathrm{i} \,.\, P_\mathrm{i}^+ \,.\, d\sigma_\mathrm{i}/d\Omega \,.\, A \tag{S2}$$

where Y_i is the scattered ion yield (from a surface atom with mass m_2), N_i is the atomic surface concentration, P_i^+ is the ion fraction (the probability that He particles scattered towards the detector will be ionised as He$^+$), $d\sigma_\mathrm{i}/d\Omega$ is the differential cross-section (element specific), I_p is the primary ion beam current, e is the elementary charge, t is the acquisition time, ξ is an instrumental factor, R is the correction factor for rough surfaces ($R = 1$ for a flat surface), and A is a constant for our experimental set-up. Y_i is measured, so to determine N_i the unknowns are P_i^+ and $d\sigma_i/d\Omega$.

8. Case study: $[C_4C_1Im][Tf_2N]$

Reproducibility: To demonstrate the reproducibility of the LEIS spectra recorded in this study, the same ionic liquid, $[C_4C_1Im][Tf_2N]$, was studied on different days (Figure S2). Both the peak energies and the peak areas are the same, within in the error of the experiment. The same reproducibility was observed for all ionic liquids in this study, demonstrating that the peak energies and in particular the peak areas for LEIS spectra for different ionic liquids are directly comparable.

Surface charging: As He^+ ions strike the ionic liquid surface, it is possible that the ionic liquid surface is left positively charged. However, a similar scenario is possible in XPS experiments (X-rays in, electrons out), and significant charging of the ionic liquid surface is most definitely not observed.[9] To confirm this finding for LEIS studies, we studied $[C_4C_1Im][Tf_2N]$ both with and without charge neutralisation (electrons are directed at the ionic liquid surface from a filament to compensate for any positive charge present at the ionic liquid surface). The LEIS spectra were the same, within the error of the experiment, confirming that surface charging is not a problem for LEIS when studying ionic liquids.

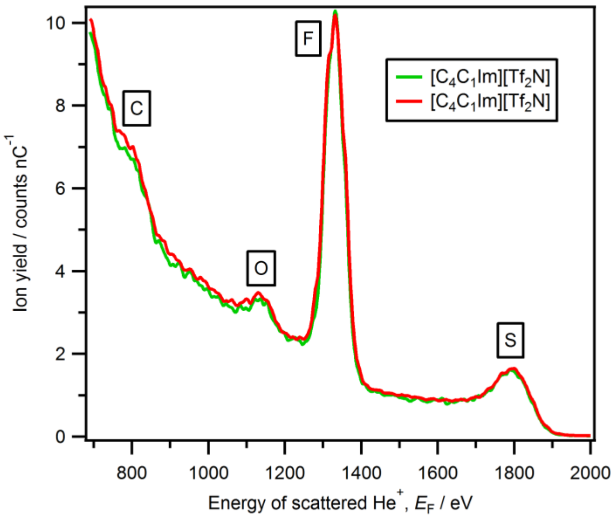

Figure S2. LEIS spectra ($^4He^+$, E_0 = 3 keV) for two different samples of $[C_4C_1Im][Tf_2N]$ recorded on different days.

Peak fitting: The archetypal element peak in a LEIS spectrum is composed of a Gaussian-shaped surface peak and an in depth tail on the lower energy side of the spectrum. The shape and intensity of the in depth tail, which is composed of a combination of several sub-surface peaks, depends upon the depth distribution of the element and the nature of the element at the outer surface which is responsible for the re-ionisation of the exiting He^0 neutrals. For common depth profiles, in which the concentration of the element in the bulk is constant, this tail is normally fitted with an error function starting ~25 eV from the main surface peak. The exact shape of this tail can be obtained by fitting a surface peak and subtracting it from the signal.[10]

In this paper we use IONTOF SurfaceLab6 LEIS data evaluation program in order to fit the LEIS spectra and determine peak energies and peak areas. The region due to each element is fitted separately, as demonstrated in Figure S3. In Figure S3c we can certainly determine that the fluorine region is a surface peak with a characteristic in-depth tail. This region can be fitted with a Gaussian peak plus an error function starting 25 eV from the Gaussian peak position. The width of the error function is set to be ±10 eV of the Gaussian peak width. In addition, an exponential decay function is fitted manually in order to account for the background. The main source of this background is sputtered ions from the sample.

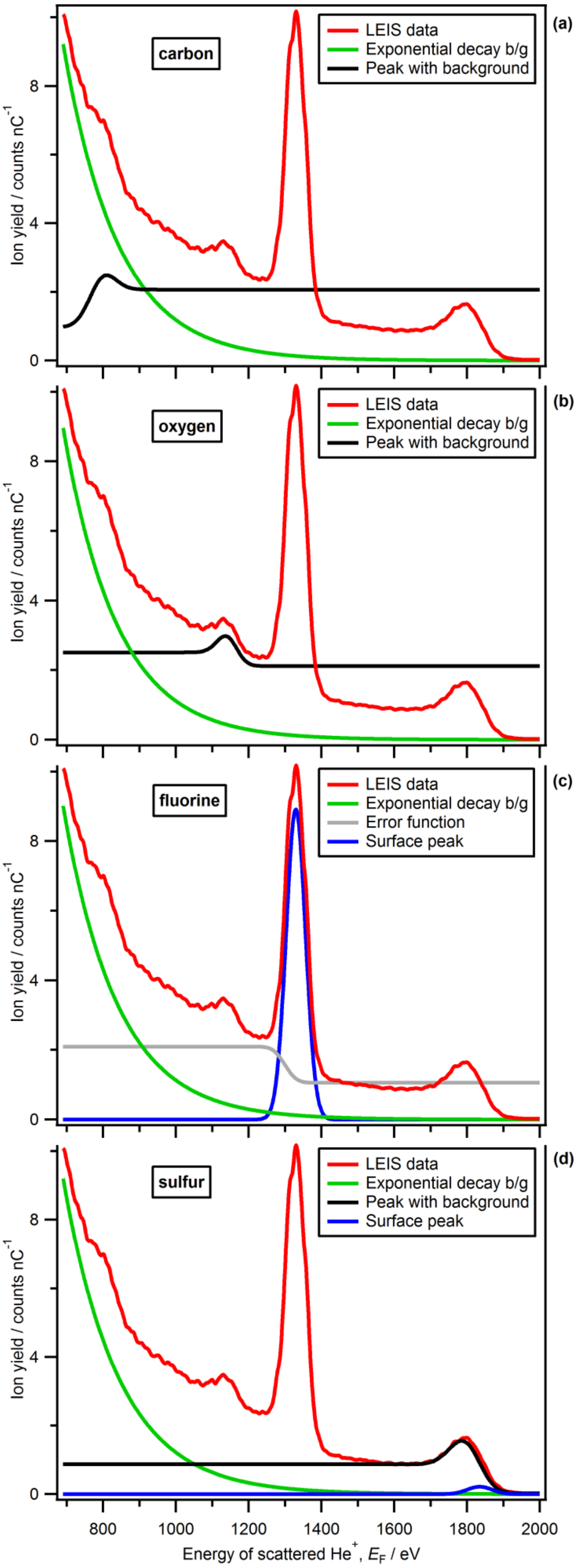

Figure S3. Fitting LEIS spectra ($^4He^+$, E_0 = 3 keV) for [C_4C_1Im][Tf_2N] recorded: (a) carbon, (b) oxygen, (c) fluorine and (d) sulfur.

The sulfur peak has a non-Gaussian shape and must have a significant sub-surface contribution. The shape is very similar to the silicon peak observed in SiO_2 sample in which 90% of the Si is covered with oxygen.[11] In our case, the origin of this shape is probably the sulfur atoms just below the oxygen atoms of the $–SO_2/SO_3$ moiety. By adding a surface peak within the fitting, $S_{Surface}$ (Gaussian peak with the same energy and width as the sulfur reference surface peak), we can fit the rest of the signal with a peak with a background function, $S_{Sub\text{-}surface}$ (Figure S3d).

The oxygen and carbon signals are too noisy to be fitted meaningfully using different surface and sub-surface peaks. Therefore, we only obtain the total area of these signals using a simple peak with background function (Figures S3a and S3b).

9. Sample purity

A number of unexpected peaks have been observed for some of the ionic liquids studied here, which are due to contamination. By far the most commonly observed contamination peaks are due to silicon and oxygen. Silicon impurities have previously been observed using XPS for a range of ionic liquids.[6, 12-16] The silicon and oxygen contamination is most likely from grease from synthesis of the ionic liquids. Three examples where silicon and oxygen contamination is present are given in Figure S4.

The first example we give is for $[C_4C_1Im][SCN]$ (Figure S4a), a commercial sample purchased from Sigma-Aldrich and used as received (apart from degassing). There are unexpected peaks due to both oxygen (1140 eV) and silicon (1714 eV, peak area = 15). These extra peaks can be removed by Ar^+ bombardment, or if studied for long enough using He^+ from LEIS (He^+ sputters surface contamination too, but slower than Ar^+ under the same conditions). When oxygen and silicon are present, the sulfur surface peak area is 58 compared to 103 for the clean $[C_4C_1Im][SCN]$ surface, a decrease of ~43%. Furthermore, the nitrogen peak has a slightly lower peak area when oxygen and silicon are present.

The second example we give is for $[C_4C_1Im][BF_4]$ (Figure S4b), a commercial sample purchased from Sigma-Aldrich and used as received. There are unexpected peaks for both oxygen (1140 eV) and silicon (1704 eV, peak area = 4). Again, a clean surface can be produced by Ar^+ bombardment. When oxygen and silicon are present, the fluorine peak is 204 compared to 248 for the clean $[C_4C_1Im][BF_4]$ surface, a decrease of ~18%.

The third example we give is for $[C_{12}C_1Im][Tf_2N]$ (Figure S4c), a sample synthesised at Imperial College London. There is an unexpected peak for silicon (1714 eV, peak area = 57); extra oxygen may be present, but such a peak would appear at a similar energy to the oxygen peak from $[C_{12}C_1Im][Tf_2N]$. A clean surface can once again be produced by Ar^+ bombardment. When silicon is present, the fluorine peak area is 8% lower and the $S_{sub\text{-}surface}$ peak area is 41% lower than for the clean $[C_{12}C_1Im][Tf_2N]$ surface. It should be noted for any ionic liquid containing phosphorus or sulfur, it is potentially difficult to determine if silicon is present, especially in small quantities, as the peaks can overlap (given their relatively similar masses).

For [$C_{12}C_1$Im][Tf_2N], the silicon peak has the largest peak area of the samples presented here with an area of 57. However, the anion peaks for this ionic liquid are dampened the least of the three ionic liquids, suggesting that the silicon-based contamination is located mainly above the cation for [$C_{12}C_1$Im][Tf_2N] but above anion for [C_4C_1Im][SCN] and [C_4C_1Im][BF_4].

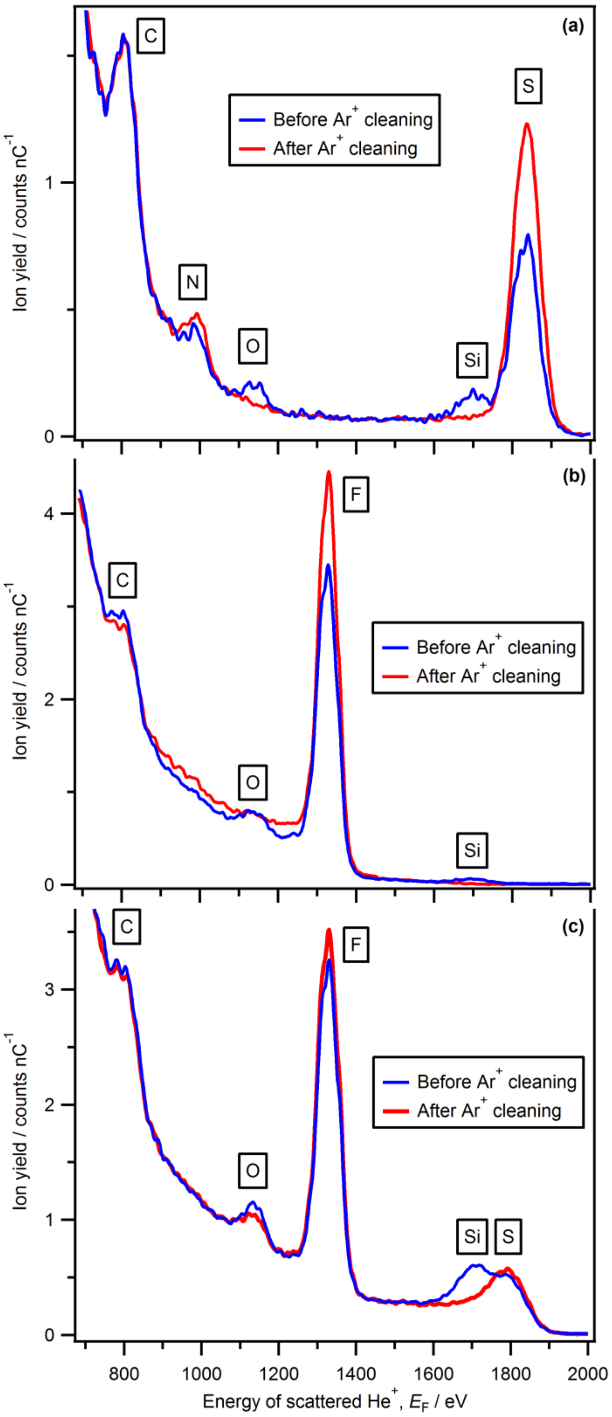

Figure S4. LEIS spectra ($^4He^+$, E_0 = 3 keV) for three ionic liquids with silicon contamination, both before and after Ar^+ bombardment: (a) [C_4C_1Im][SCN], (b) [C_4C_1Im][BF_4], (c) [$C_{12}C_1$Im][Tf_2N].

For these three samples, once the contamination had been removed, no more contamination was observed. However, for some ionic liquid samples, we did observe contamination being removed from the outer surface to give a clean LEIS spectrum, but with more returning over time. This behaviour is similar to how a traditional surfactant behaves in water; a certain amount of surfactant can be present at the outer surface and if there is more surfactant present in the sample, it remains in the bulk. Based upon the silicon peak areas, we estimate that ~10% of the outer surface is composed of silicon-based contamination. *i.e.* ~10^{14} atoms cm^{-2}. For these LEIS experiments, the sample surface area is ~1 cm^2 (*i.e.* ~10^{14} contamination atoms per sample), and we use ~0.3 ml for each sample studied (*i.e.* ~10^{20} to 10^{21} ionic liquid ion pairs in the sample). Detecting 10^{14} silicon atoms per 10^{20} ionic liquid ion pairs is challenging using traditional bulk scale techniques such as NMR. Therefore, when non-element specific techniques such as X-ray reflectivity (XRR) are employed to study ionic liquid-gas surfaces, caution must be taken as sample purity cannot be accurately determined. It is recommended, if possible, that *in situ* Ar^+ bombardment is used to clean the ionic liquid-gas surface before conducting experiments, as it has been clearly demonstrated that Ar^+ bombardment does not lead to long-term sample damage.

Kauling *et al*. used LEIS to investigate the distribution of gold nanoparticles in $[C_4C_1Im][PF_6]$ and four functionalised ionic liquids. Their LEIS spectra reveal that some of their ionic liquids, *e.g.* $[C_4C_1Im][PF_6]$, were heavily contaminated with silicon and oxygen impurities. Indeed, for one ionic liquid, $[C_{2SH}C_1Im][PF_6]$ ($[C_{2SH}C_1Im]^+$ = 1-(2-thio-ethyl)-3-methylimidazolium), by our judgement the only peaks observed are due to carbon, oxygen and silicon, with no significant fluorine or sulfur peaks, indicative of the outer surface being dominated by silicon grease to such an extent that the ionic liquid is almost, if not entirely, hidden. Conclusions on the ionic liquid-gas surface structure for such contaminated ionic liquid samples should be treated with extreme caution.

It should be noted that there is also a very small chlorine peak at ~1905 eV for $[C_2C_1Im][N(CN)_2]$ and $[C_4C_1Im][N(CN)_2]$, both of which are commercially purchased samples from Sigma-Aldrich, and used as received (apart from degassing). The peak areas are both <1.5, much smaller than the Cl peak area for $[P_{6,6,6,14}]Cl$. These chlorine peaks were not removed by Ar^+ bombardment, indicating that the chlorine contamination was present in the bulk ionic liquid at similar concentrations to its presence at the outer surface, not as a surfactant-type contaminant that could be removed by sputtering.

For $[C_4C_1Im][C_0OSO_3]$, a very small fluorine peak is observed at 1325 eV in the LEIS spectrum presented in Figure 7; the peak area is very small, 1.8. We expect this peak is due to adsorption from the gas phase of a small amount of fluorine-based contamination, most likely produced when we studied $[C_4C_1Im][Tf_2N]$ shortly before. Similar fluorine contamination was observed for a solid sample in another study at a similar time, further endorsing our explanation. This contamination is likely to affect the peak areas very slightly for $[C_4C_1Im][C_0OSO_3]$; however, the presence of this fluorine contamination does not affect any of the conclusions made in this paper for $[C_4C_1Im][C_0OSO_3]$.

Overall, our ionic liquids are generally high purity (20 of the 23 ionic liquids studied here gave clean surfaces), and we have studied a large number composed of a variety of different cations and anions.

10. Analysing LEIS spectra: elemental quantification

Ionic liquid	C	N	O	F	P	$S_{\mathrm{sub\text{-}surface}}$	S_{surface}	Cl
[C$_4$C$_1$Im][CF$_3$SO$_3$]	799		1138	1329		1795	1835	
[C$_4$C$_1$Im][PF$_6$]	790			1327	1784			
[C$_4$C$_1$Im][BF$_4$]	806			1328				
[C$_2$C$_1$Im][Tf$_2$N]	786		1140	1330		1795	1835	
[C$_4$C$_1$Im][Tf$_2$N]	790		1141	1330		1797	1835	
[C$_6$C$_1$Im][Tf$_2$N]	792		1138	1330		1795	1835	
[C$_8$C$_1$Im][Tf$_2$N]	800		1138	1330		1795	1835	
[C$_{12}$C$_1$Im][Tf$_2$N]	798		1137	1328		1792	1835	
[C$_4$C$_1$Pyrr][Tf$_2$N]	786		1139	1328		1797	1835	
[N$_{4,1,1,1}$][Tf$_2$N]	793		1137	1327		1795	1835	
[P$_{6,6,6,14}$][Tf$_2$N]	801		1135	1328		1793	1835	
[P$_{6,6,6,14}$]Cl	809				1783			1897
[C$_8$C$_1$Im]Cl	807							1904
[P$_{6,6,6,14}$][N(CN)$_2$]	819	1003			1787			
[C$_2$C$_1$Im][N(CN)$_2$]	814	997						
[C$_4$C$_1$Im][N(CN)$_2$]	811	996						
[C$_2$C$_1$Im][B(CN)$_4$]	810	997						
[C$_4$C$_1$Im][SCN]	810	992					1835	
[C$_4$C$_1$Im][C$_0$OSO$_3$]	808		1140			1811	1835	
[C$_4$C$_1$Im][C$_1$OSO$_3$]	808		1139			1797	1835	
[C$_4$C$_1$Im][C$_8$OSO$_3$]	809		1141			1798	1835	
[C$_2$C$_1$Im][C$_1$CO$_2$]	816	987	1143					
[C$_4$C$_1$Im][C$_1$CO$_2$]	811		1140					
Clean diamond	809							
Oxygen-covered diamond			1142					

Table S3. Peak energies for all ionic liquids in this study in eV.

Ionic liquid	C	N	O	F	P	$S_{sub\text{-}surface}$	$S_{surface}$	Cl
$[C_4C_1Im][CF_3SO_3]$	74		58	449		103	12	
$[C_4C_1Im][PF_6]$	64			540	127			
$[C_4C_1Im][BF_4]$	42			248				
$[C_2C_1Im][Tf_2N]$	65		86	709		165	36	
$[C_4C_1Im][Tf_2N]$	64		55	571		137	18	
$[C_6C_1Im][Tf_2N]$	65		46	475		112	15	
$[C_8C_1Im][Tf_2N]$	60		36	371		88	12	
$[C_{12}C_1Im][Tf_2N]$	62		17	204		50	5	
$[C_4C_1Pyrr][Tf_2N]$	51		50	569		150	6	
$[N_{4,1,1,1}][Tf_2N]$	50		52	547		142	10	
$[P_{6,6,6,14}][Tf_2N]$	58		15	187		48	4	
$[P_{6,6,6,14}]Cl$	36				4			9
$[C_8C_1Im]Cl$	55							21
$[P_{6,6,6,14}][N(CN)_2]$	50	4			4			
$[C_2C_1Im][N(CN)_2]$	69	72						
$[C_4C_1Im][N(CN)_2]$	57	46						
$[C_2C_1Im][B(CN)_4]$	92	164						
$[C_4C_1Im][SCN]$	52	13					103	
$[C_4C_1Im][C_0OSO_3]$	60		78			41	19	
$[C_4C_1Im][C_1OSO_3]$	48		61			42	14	
$[C_4C_1Im][C_8OSO_3]$	49		11			9	2	
$[C_2C_1Im][C_1CO_2]$	65	7	40					
$[C_4C_1Im][C_1CO_2]$	50		20					

Table S4. Peak areas for all ionic liquids in this study.

11. Stoichiometric amounts of each element in all 23 ionic liquids studied

	Number of type of element present in ionic liquid										Percentage of type of element present in the ionic liquid (excluding hydrogen)										M(CA)	ρ	V_{mol}
Ionic liquid	C_{cation}	C_{anion}	N_{cation}	N_{anion}	P	O	S	F	B	Cl	C_{cation}	C_{anion}	N_{cation}	N_{anion}	P	O	S	F	B	Cl	g mol^{-1}	g cm^{-3}	nm^3
$[C_4C_1Im][CF_3SO_3]$	8	1	2			3	1	3			44	6	11			17	6	17			288.3	1.30 [17]	0.369
$[C_4C_1Im][PF_6]$	8		2		1			6			47		12		6			35			284.2	1.37 [18]	0.345
$[C_4C_1Im][BF_4]$	8		2					4	1		53		13					27	7		226.1	1.19 [18]	0.316
$[C_2C_1Im][Tf_2N]$	6	2	2	1		4	2	6			26	9	9	4		17	9	26			391.4	1.52 [19]	0.427
$[C_4C_1Im][Tf_2N]$	8	2	2	1		4	2	6			32	8	8	4		16	8	24			419.4	1.44 [18]	0.486
$[C_6C_1Im][Tf_2N]$	10	2	2	1		4	2	6			37	7	7	4		15	7	22			447.5	1.36 [18]	0.545
$[C_8C_1Im][Tf_2N]$	12	2	2	1		4	2	6			41	7	7	3		14	7	21			475.5	1.31 [18]	0.603
$[C_{12}C_1Im][Tf_2N]$	16	2	2	1		4	2	6			48	6	6	3		12	6	18			531.7	1.24 [18]	0.710
$[C_4C_1Pyrr][Tf_2N]$	9	2	1	1		4	2	6			36	8	4	4		16	8	24			422.5	1.39 [18]	0.503
$[N_{4,1,1,1}][Tf_2N]$	7	2	1	1		4	2	6			30	9	4	4		17	9	26			396.4	1.37 [20]	0.479
$[P_{6,6,6,14}][Tf_2N]$	32	2		1	1	4	2	6			67	4		2	2	8	4	13			764.1	1.05 [20]	1.209
$[P_{6,6,6,14}]Cl$	32				1					1	94				3					3	519.4	0.88 [20]	0.978
$[C_8C_1Im]Cl$	12		2							1	80		13							7	230.8	1.01 [18]	0.380
$[P_{6,6,6,14}][N(CN)_2]$	32	2		3	1						84	5		8	3						550.0	0.90 [21]	1.016
$[C_2C_1Im][N(CN)_2]$	6	2	2	3							46	15	15	23							177.2	1.11 [22]	0.266
$[C_4C_1Im][N(CN)_2]$	8	2	2	3							53	13	13	20							205.3	1.06 [22]	0.322
$[C_2C_1Im][B(CN)_4]$	6	4	2	4					1		35	24	12	24					6		226.1	1.04 [23]	0.362
$[C_4C_1Im][SCN]$	8	1	2	1			1				62	8	15	8			8				197.3	1.07 [24]	0.306
$[C_4C_1Im][C_0OSO_3]$	8		2			4	1				53		13			27	7				236.3	1.28 [25]	0.308
$[C_4C_1Im][C_1OSO_3]$	8	1	2			4	1				50	6	13			25	6				250.4	1.21 [26]	0.343
$[C_4C_1Im][C_8OSO_3]$	8	8	2			4	1				35	35	9			17	4				348.6	1.06 [27]	0.544
$[C_2C_1Im][C_1CO_2]$	6	2	2			2					50	17	17			17					170.2	1.10 [28]	0.257
$[C_4C_1Im][C_1CO_2]$	8	2	2			2					57	14	14			14					198.3	1.05 [29]	0.313

Table S5. Stoichiometric amounts of each element in all 23 ionic liquids studied. Ionic liquid densities, ρ, to obtain ionic liquid ion pair molecular volumes, V_{mol}, are taken from references [17-29].

As at present we cannot present full composition analysis of the outer surface of the ionic liquids using our LEIS data, we need a method to judge whether the changes in the LEIS spectra with *n* are in line with changes in the stoichiometry of the ionic liquids, or whether the changes demonstrate surface structuring. We use the value (as %) based upon the number of each type of atom (*e.g*. $[C_4C_1Im][C_0OSO_3]$ contains four oxygen atoms) relative to the total number of non-hydrogen atoms (*e.g*. $[C_4C_1Im][C_0OSO_3]$ contains 15 non-hydrogen atoms) as a method to compare to the results from our LEIS spectra. (*i.e*. number of each type of atom relative to the total number of non-hydrogen atoms). It is important to note that changing *n* for $[C_nC_1Im][Tf_2N]$ does not have a dramatic impact upon the percentage of anion atoms in the bulk ionic liquid. For example, $[C_2C_1Im][Tf_2N]$ contains 26% F atoms and $[C_{12}C_1Im][Tf_2N]$ contains 18% F atoms, a decrease of only 8% as 10 CH_2 units are added. Therefore, if the outer surface composition reflects the bulk composition then the LEIS anionic peak areas would decrease only relatively little.

References

1. A. E. Bradley, C. Hardacre, J. D. Holbrey, S. Johnston, S. E. J. McMath and M. Nieuwenhuyzen, *Chem. Mat.*, 2002, **14**, 629-635.
2. A. Brandt, M. J. Ray, T. Q. To, D. J. Leak, R. J. Murphy and T. Welton, *Green Chem.*, 2011, **13**, 2489-2499.
3. H. H. Brongersma, M. Draxler, M. de Ridder and P. Bauer, *Surf. Sci. Rep.*, 2007, **62**, 63-109.
4. H. H. Brongersma, in *Characterization of materials*, ed. E. N. Kaufmann, Wiley, 2nd edn., 2012, pp. 1-23.
5. H. R. J. ter Veen, T. Kim, I. E. Wachs and H. H. Brongersma, *Catal. Today*, 2009, **140**, 197-201.
6. C. Kolbeck, M. Killian, F. Maier, N. Paape, P. Wasserscheid and H. P. Steinrück, *Langmuir*, 2008, **24**, 9500-9507.
7. K. R. J. Lovelock, I. J. Villar-Garcia, F. Maier, H. P. Steinrück and P. Licence, *Chem. Rev.*, 2010, **110**, 5158-5190.
8. M. Lísal, Z. Posel and P. Izák, *Phys. Chem. Chem. Phys.*, 2012, **14**, 5164-5177.
9. I. J. Villar-Garcia, E. F. Smith, A. W. Taylor, F. L. Qiu, K. R. J. Lovelock, R. G. Jones and P. Licence, *Phys. Chem. Chem. Phys.*, 2011, **13**, 2797-2808.
10. F. J. J. Janssen, L. J. van Ijzendoorn, A. W. D. van der Gon, M. J. A. de Voigt and H. H. Brongersma, *Phys. Rev. B*, 2004, **70**, 11.
11. T. Janssens, C. Huyghebaert, W. Vandervorst, A. Gildenpfennig and H. H. Brongersma, *Appl. Surf. Sci.*, 2003, **203**, 30-34.
12. E. F. Smith, F. J. M. Rutten, I. J. Villar-Garcia, D. Briggs and P. Licence, *Langmuir*, 2006, **22**, 9386-9392.
13. K. R. J. Lovelock, E. F. Smith, A. Deyko, I. J. Villar-Garcia, P. Licence and R. G. Jones, *Chem. Commun.*, 2007, 4866-4868.
14. J. M. Gottfried, F. Maier, J. Rossa, D. Gerhard, P. S. Schulz, P. Wasserscheid and H. P. Steinrück, *Z. Phys. Chemie-Int. J. Res. Phys. Chem. Chem. Phys.*, 2006, **220**, 1439-1453.
15. C. Kolbeck, T. Cremer, K. R. J. Lovelock, N. Paape, P. S. Schulz, P. Wasserscheid, F. Maier and H. P. Steinrück, *J. Phys. Chem. B*, 2009, **113**, 8682-8688.
16. K. R. J. Lovelock, C. Kolbeck, T. Cremer, N. Paape, P. S. Schulz, P. Wasserscheid, F. Maier and H. P. Steinrück, *J. Phys. Chem. B*, 2009, **113**, 2854-2864.
17. M. Deetlefs, K. R. Seddon and M. Shara, *Phys. Chem. Chem. Phys.*, 2006, **8**, 642-649.
18. H. Jin, B. O'Hare, J. Dong, S. Arzhantsev, G. A. Baker, J. F. Wishart, A. J. Benesi and M. Maroncelli, *J. Phys. Chem. B*, 2008, **112**, 81-92.
19. A. P. Fröba, H. Kremer and A. Leipertz, *J. Phys. Chem. B*, 2008, **112**, 12420-12430.
20. P. Kilaru, G. A. Baker and P. Scovazzo, *J. Chem. Eng. Data*, 2007, **52**, 2306-2314.
21. A. B. Pereiro, H. I. M. Veiga, J. Esperanca and A. Rodriguez, *J. Chem. Thermodyn.*, 2009, **41**, 1419-1423.
22. J. Klomfar, M. Součková and J. Pátek, *J. Chem. Eng. Data*, 2011, **56**, 3454-3462.
23. T. Koller, M. H. Rausch, P. S. Schulz, M. Berger, P. Wasserscheid, I. G. Economou, A. Leipertz and A. P. Fröba, *J. Chem. Eng. Data*, 2012, **57**, 828-835.
24. U. Domanska and M. Laskowska, *J. Chem. Eng. Data*, 2009, **54**, 2113-2119.
25. B. Yoo, W. Afzal and J. M. Prausnitz, *J. Chem. Thermodyn.*, 2013, **57**, 178-181.
26. J. S. Torrecilla, J. Palomar, J. Garcia and F. Rodriguez, *J. Chem. Eng. Data*, 2009, **54**, 1297-1301.
27. A. Wandschneider, J. K. Lehmann and A. Heintz, *J. Chem. Eng. Data*, 2008, **53**, 596-599.
28. A. P. Fröba, M. H. Rausch, K. Krzeminski, D. Assenbaum, P. Wasserscheid and A. Leipertz, *Int. J. Thermophys.*, 2010, **31**, 2059-2077.
29. H. F. D. Almeida, H. Passos, J. A. Lopes-da-Silva, A. M. Fernandes, M. G. Freire and J. A. P. Coutinho, *J. Chem. Eng. Data*, 2012, **57**, 3005-3013.